Fuel Processing Technology, Volume 222, November 2021, Article number 106976
DOI:10.1016/j.fuproc.2021.106976

Kinetic Study and Modeling on the Regeneration of Li_4SiO_4-based Sorbents for High-Temperature CO_2 Capture

Shuzhen Chen [a], *Changlei Qin* [a,*], *Weiyang Yuan* [a], *Dawid P. Hanak* [b], *and Jingyu Ran* [a]

[a] Key Laboratory of Low-grade Energy Utilization Technologies and Systems of Ministry of Education, School of Energy and Power Engineering, Chongqing University, Chongqing 400044, China

[b] Energy and Power Theme, School of Water, Energy and Environment, Cranfield University, Bedford, Bedfordshire MK43 0AL, UK

Abstract

Li_4SiO_4 is acknowledged as a promising sorbent candidate in high-temperature CO_2 adsorption. However, reaction kinetics for the regeneration process of Li_4SiO_4, especially its dependence on CO_2 pressure is lack of understanding. This work designed and carried out a series of isothermal tests on the regeneration of pure Li_4SiO_4 and K-Li_4SiO_4 under CO_2 partial pressure of 0-0.5 atm and temperature of 625-725 °C. For the first time, the expression of $(P_{eq}-P_{CO_2})^n$ is introduced into the regeneration rate equation so as to reveal its dependence on CO_2 pressure. The reaction order (n) is found to grade according to the value of $(P_{eq}-P_{CO_2})$, and the apparent activation energy is calculated as 284.42 kJ•mol^{-1} and 146.31 kJ•mol^{-1} for the regeneration of Li_4SiO_4 and K-Li_4SiO_4, respectively. Furthermore, this work proposes that power law model with m=4/3 is the most probable mechanism function for the regeneration of Li_4SiO_4-based sorbents.

Keywords: high-temperature CO_2 capture, CO_2 adsorption and desorption, Li_4SiO_4, regeneration kinetics.

* Corresponding author. Email: c.qin@cqu.edu.cn.

1. Introduction

High-temperature adsorption is an efficient way to separate CO_2 from tail gas in various industrial fields. Typical CO_2 sorbents under high-temperature circumstances include calcium-based *(1-3)* and lithium-based materials *(4-6)*. Due to the good carbon capture capacity and cyclic durability, Li_4SiO_4 has been widely investigated as a potential high-temperature CO_2 sorbent in recent years *(7)*. Actually it can be used in both the temperature swing adsorption (TSA) and pressure swing adsorption (PSA), following the reversible chemical reactions of Eq. 1, though more work is focused on the former in the literature *(8)*. Under the TSA context, the adsorption temperature basically ranges in 500-715 °C *(9, 10)* and desorption in 700-850 °C *(10, 11)*, and the swing border between adsorption and desorption obeys the thermodynamic equilibrium correlation of temperature and CO_2 pressure.

$$Li_4SiO_4 + CO_2 \rightleftharpoons Li_2SiO_3 + Li_2CO_3 \quad (1)$$

The theoretical CO_2 adsorption capacity by Li_4SiO_4 reaches up to 0.367 g/g sorbents. However, the practical capacity is strongly dependent on sorbents characteristics, reaction temperatures/pressures, and foreign gases like H_2S/SO_2 *(12-16)*. Till now, a lot of work has been conducted on the improvement of CO_2 capacity and cyclic stability, involving synthesis routes adaptation *(17, 18)*, Li/Si precursors selection *(5, 18)*, physical-chemical modification *(19-23)*. Meanwhile, some investigate the reaction mechanisms and kinetics, so as to clarify the kinetic limit (chemical reaction or molecule/ion diffusion) *(8, 11)*. In particular, doping of alkaline carbonates is an effective method to improve both CO_2 adsorption capacity and reaction kinetics of Li_4SiO_4. As early as 2002. Kato et al. *(24)* reported the positive effect of K_2CO_3 to CO_2 adsorption by Li_4SiO_4. Hu et al. *(25)* firstly detected the endothermic peak at ~500 °C, verifying a melting process during CO_2 adsorption by K_2CO_3-doped Li_4SiO_4.

Several kinetic models like double exponential model *(6, 10, 26)*, Avrami–Erofeev model *(10, 17)* and shrinking core model *(17, 27, 28)* have been used to describe the adsorption process under various temperatures and gas concentrations. However, only the modified Jander model was reported to best cope with the effect of steam and CO_2 pressure during adsorption *(29)*. Regarding to the desorption process,

the kinetic study is very scarce and insufficient *(9, 10, 30)*. To be specific, Qi et al. *(10)* reported that the Avrami–Erofeev model, together with the double-shell mechanism could be used for analyzing the isothermal CO_2 desorption in 650-750 °C. Later, Quddus et al. *(30)* used a Nucleation and Nuclei Growth Model (NNGM) to simulate the non-isothermal CO_2 desorption process of an acid treated Li_4SiO_4, and concluded that the CO_2 desorption rate was ruled by the formation and three dimensional growths of nuclei. More recently, Amorim et al. *(9)* studied the regeneration of Li_4SiO_4 by shrinking core model for the first time. Despite there are good fitting results towards the desorption of carbonated Li_4SiO_4, the gas atmosphere is idealized as pure N_2. Considering that sorbents are surely regenerated under a CO_2-containing atmosphere in practical applications *(31)*, the regeneration kinetics of Li_4SiO_4 under various CO_2 concentrations deserves further investigation and in-depth understanding.

A kinetic model with the most probable mechanism function is greatly effective in assisting the in-depth kinetic analysis, i.e. identifying the rate-limiting stage in a gas-solid reaction, which is pivotal to the reaction efficiency. For the adsorption process of Li_4SiO_4, it is acknowledged that the rate-limiting stage is the diffusion of CO_2 or Li^+/O^{2-} across the product layer *(32-35)*, thus the representative diffusion-controlled Jander model could properly describe the adsorption process *(36)*. Comparing to adsorption, CO_2 desorption from the carbonated Li_4SiO_4 has a much quicker reaction rate, and is considered to be controlled by the formation and growth of Li_4SiO_4 crystals *(10)*. In general, shrinking core model has the strongest mechanistic basis *(7)*, and three factors are considered in the form of resistance parameters: the external mass transfer, product layer diffusion and chemical reaction *(9, 17)*. But the complicated formula raises difficulty for data fitting. The Avrami-Erofeev model has a simpler expression, and distinguishes the chemical reaction-controlled and diffusive reaction-controlled stage by the value of '*n*', but lacks clear physical interpretation *(9)*. Power law model has been widely applied to gas-solid reaction, and has the biggest advantage of simplicity to reconcile the experimental data *(37, 38)*. Although the selection of exponential is relatively empirical, the abundant references could provide suggestive range of selection. Additionally, the comparison among different exponentials is quick and clear. Considering the simplicity

and applicability, power law model is applied to investigate the intrinsic regeneration kinetics of Li_4SiO_4 in the work.

To reveal characteristics of the CO_2 desorption process under various conditions, especially understanding the key role of CO_2 pressure, here we present a kinetic study on the regeneration of Li_4SiO_4-based sorbents. Various techniques of X-Ray diffraction (XRD), N_2 sorption/desorption, scanning electron microscope (SEM), energy disperse spectroscopy (EDS), and thermogravimetry (TG) were utilized to show features of Li_4SiO_4 and K-Li_4SiO_4. In general, the reaction order to $(P_{eq}-P_{CO_2})$ and apparent activation energies were obtained by analyzing desorption rates in the initial linear profile. Besides, the intrinsic activation energy of the overall reaction was calculated through conversion-time fitting by power law model.

2. Experimental

2.1. Samples Preparation

In this work, Li_4SiO_4-based sorbents were synthesized through a typical solid-state method, using raw materials of Li_2CO_3 and SiO_2. Additionally, K_2CO_3 was adopted as an alkali metal carbonate dopant. All raw materials, lithium carbonate (Li_2CO_3, ≥99.0% purity), fumed silica (SiO_2, 150 m^2/g, lyophobic), and potassium carbonate (K_2CO_3, analytically pure) were purchased from Shanghai Aladdin Biochemical Technology Co., Ltd.

During sorbents synthesis, lithium and silica precursor were weighted in a molar ratio of Li:Si=4.1:1, where an excess 0.1 for lithium took account for the possible sublimation of Li_2CO_3. Then, the materials were fully mixed in a planetary ball mill (XQM-2) with zirconia beads for 65 min at a speed of 400 rpm, by rotating clockwise for 10 min and then reverse for the same time with intervals of 30 s in between. Next, the blended materials were calcined at 750 °C for 6 h in a muffle furnace, following by trituration and sieving to obtain Li_4SiO_4 with particle size ranging in 75-106 μm. For K_2CO_3-doped Li_4SiO_4

(abbreviated as K-Li_4SiO_4), the only difference was the original molar ratio of Li:Si:K=4.1:1:0.1, and all preparation steps were kept the same.

2.2. Materials Characterization

X-ray diffractometer (Spectris Pte. Ltd, PANalytical X' Pert Powder) was used to identify the specific chemical phases in the synthetic sorbents, with Cu radiation at 50 kV and 55 mA, scanning from 10° to 80° for 20 min. Surface morphology of sorbents was examined through an environmental scanning electron microscope (Thermo Scientific, Quattro S) with an acceleration voltage of 20 kV and 15 kV. Surface element distribution was analyzed through an energy dispersive spectrometer (Thermo Scientific, X-act compact). Surface area, pore volume and pore size distribution were obtained by the Brunauer-Emmett-Teller (BET) and Barrett-Joyner-Halenda (BJH) method in an automatic multi-station analyzer (Quantachrome Instruments, Quadrasorb 2MP) via N_2 sorption/desorption isotherms after out-gassing under vacuum for 8 h at 160 °C.

2.3. Thermogravimetric Analysis

Both the cyclic performance and desorption rate were tested in a thermogravimetric analyzer (Netzsch TG 209 F3) under a constant total pressure of 1 atm.

Cyclic test: To demonstrate the performance of synthetic sorbents, 10 cycles of adsorption and desorption were carried out in the TG analyzer. The sorbent was first heated to 700 °C and kept for 10 min to remove any possible steam or CO_2. After cooling to 650 °C, adsorption was performed in 0.5 atm CO_2 (N_2 as balance) for 30 min, followed by desorption at 700 °C in pure N_2 for 10 min.

Desorption test: To improve the experimental efficiency and consistency, sorbents were preliminarily carbonated in a tubular furnace to adsorb pure CO_2 at 600 °C for 5 h, under a gas flow rate of 2 L/min. After that, the carbonated sample was loaded in the TG analyzer for desorption tests under various CO_2 pressures and temperatures. To study the effect of CO_2 pressure, 10 mg carbonated sample was heated in pure CO_2 to 700 °C at a rate of 40 °C/min, and then CO_2 partial pressure was switched to 0-0.5 atm (N_2 as balance) for CO_2 desorption. For the effect of temperature, the same sample was heated in pure CO_2 to

a target temperature of 625-725 °C at a rate of 40 °C/min, then the atmosphere was switched to pure N_2. All isothermal desorption tests lasted for 30 min.

In this work, the desorption conversion is defined as:

$$X = \frac{m_0 - m_t}{\Delta m_{\max}} \tag{2}$$

where m_0 represents the weight at the beginning of desorption, m_t represents the real-time weight, and Δm_{max} is the amount of CO_2 adsorbed in the equivalent sample during tube furnace carbonation.

2.4. Kinetics Evaluation

In this work, the analysis of desorption kinetics involves two aspects, namely, the apparent reaction characteristics through initial reaction rate modeling and the intrinsic reaction characteristics through overall power-law modeling. The former takes the regeneration of CaO-based sorbents as reference, where the initial apparent reaction rate is proportional to $(P_{eq}\text{-}P_{CO_2})^n$ *(9, 37)*. Thus, the expression for the regeneration of Li_4SiO_4-based sorbents is presented as Eq. 3, and the calculation of theoretical CO_2 equilibrium pressure follows Eq. 4 *(39)*.

$$-r_A = k_0 \cdot \exp(\frac{-E_a}{RT}) \cdot (P_{eq} - P_{CO_2})^n \tag{3}$$

$$\ln \frac{P_{eq}}{101325} = \frac{-14414.24}{T} + 14.77 \tag{4}$$

where, r_A is the reaction rate (s^{-1}), X is the reaction conversion, k_0 represents the frequency factor ($Pa^{-n}s^{-1}$), E_a is the activation energy ($J \cdot mol^{-1}$), R is the gas constant (8.314 $J \cdot mol^{-1}K^{-1}$), and n indicates the reaction order.

In addition, a mathematical reaction model as shown of Eq. 5 is adopted to understand the CO_2 desorption process, where K is the reaction rate constant (s^{-1}):

$$\frac{dX}{dt} = K \cdot F(X) \tag{5}$$

The mechanism function, *F(X),* has different forms according to gas-solid reaction kinetic models, and the most probable mechanism function could best fit the experimental results *(10, 27)*. For example, the

power law models suggest an expression of $F(X)=(1-X)^m$, with m being an empirical parameter, varying from 0 to 10 to fit with experimental data *(10)*. It is reported that m can be identified as a shape factor that varies with the geometry of the grains, or an order of reaction *(40)*. According to the carbonation and regeneration of CaO sorbents, m=2/3 is frequently used when the process is chemical reaction-controlled, while m=4/3 is suited to the diffusion-controlled process *(38)*.

3. Results and Discussion

3.1. Sorbents Characteristic and Performance

To obtain physical and chemical characteristics of Li_4SiO_4 and K-Li_4SiO_4, comprehensive techniques including XRD, BET-BJH, SEM-EDS, and cyclic adsorption/desorption were carried out. XRD patterns in Fig. 1 (a) show that the main peaks in sample Li_4SiO_4 and K-Li_4SiO_4 are Li_4SiO_4 (PDF#76-1085 *(41)*), along with some peaks of Li_2SiO_3 and Li_2CO_3, which is very likely to be caused by the excess lithium in the precursor, or adsorption of environmental CO_2. In addition, no peak of K_2CO_3 or $LiKCO_3$ is detected, possibly due to the low content or poor crystallinity *(42)*. N_2 isotherms of both sorbents in Fig. 1 (b) have a hysteresis loop of type H3, indicating the aggregation of plate-like particles forming slit-like pores *(43)*. Fig. 1 (c) compares the specific surface area, pore volume and pore diameter of two samples, to find that their pore volumes are almost the same. The surface area of pure Li_4SiO_4 (1.638 m^2/g) is slightly smaller than K-Li_4SiO_4 (2.193 m^2/g), both within the reported range of 1-5 m^2/g in the literature *(12, 18)*. Additionally, Fig. 1 (d) shows that the size of most pores locates in 3-5 nm for both samples.

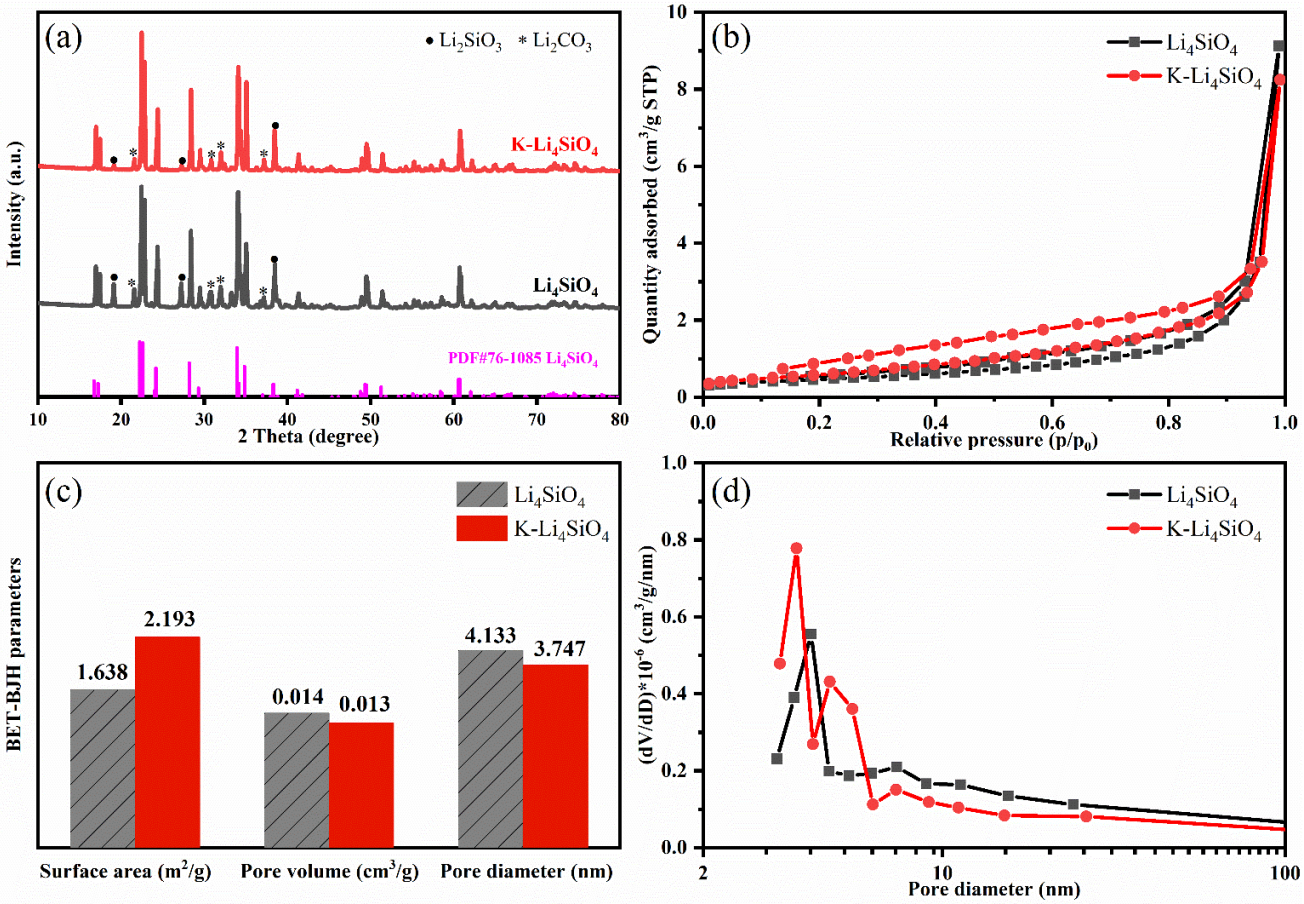

Figure 1. Characteristics of sorbents: (a) XRD, (b) N_2 adsorption/desorption isotherms, (c) surface area, pore volume and pore diameter, and (d) pore-size distribution.

Fig. 2 demonstrates the microscopic morphologies of Li_4SiO_4 and K-Li_4SiO_4. Obviously, both samples are composed of irregular granular particles, while the latter appears to be much coarser on the surface than the former, and tends to agglomerate as well. This phenomenon is thought to be caused by the eutectic effect during sorbent preparation, as Li/K eutectic carbonates could appear over 500 °C and disappear after cooling down *(42)*. EDS mapping suggests a uniform distribution of Si element in both samples, and K element in K-Li_4SiO_4. Fig. 3 depicts the CO_2 adsorption/desorption feature of the sorbents. The initial decrease of mass to 89% is due to the release of impurities like steam and CO_2 in sorbents. Similar to the adsorption process, desorption can be divided into the fast reaction stage and the slow diffusion stage as well, which in some extent indicates that an analogous kinetic study approach is applicable. Not

surprisingly, K-Li_4SiO_4 owns a much higher adsorption capacity (~0.2 g/g sorbent) than that of pure Li_4SiO_4 (~0.04 g/g sorbent).

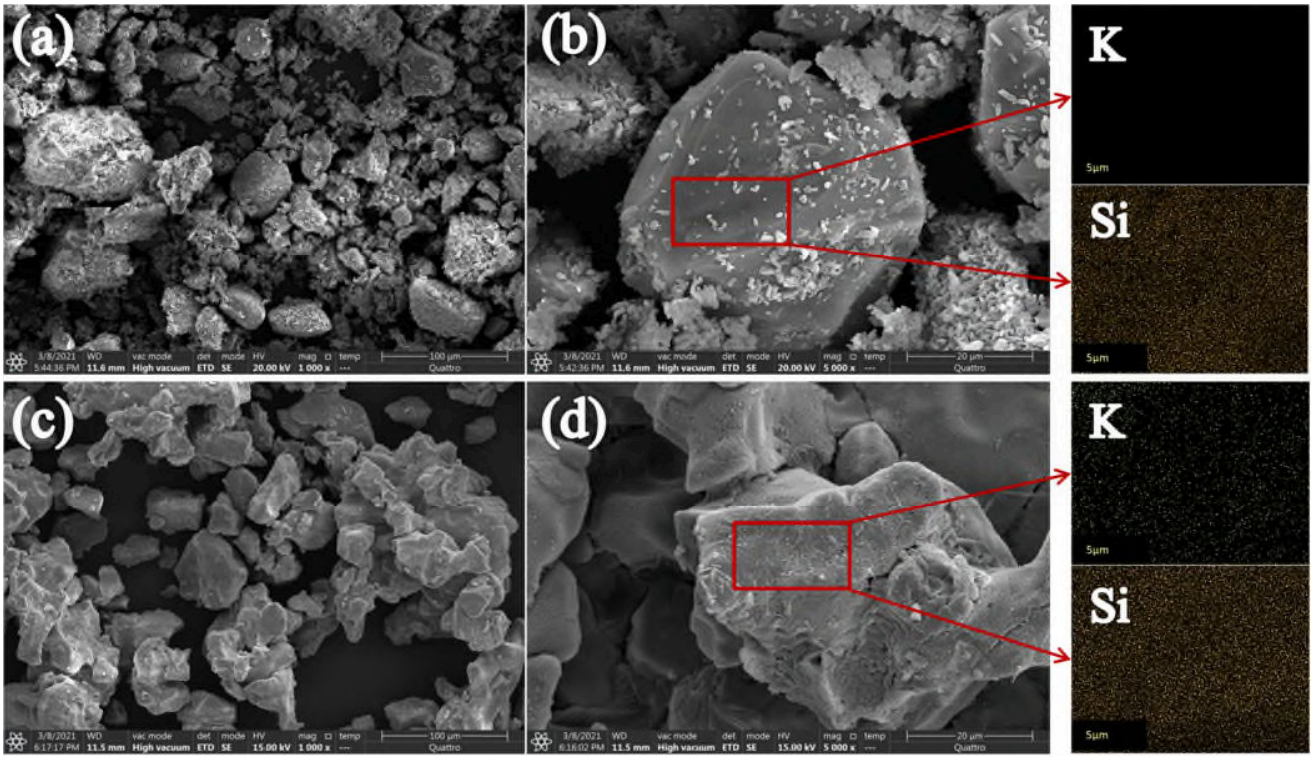

Figure 2. SEM morphology and EDS mapping of (a, b) Li_4SiO_4 and (c, d) K-Li_4SiO_4.

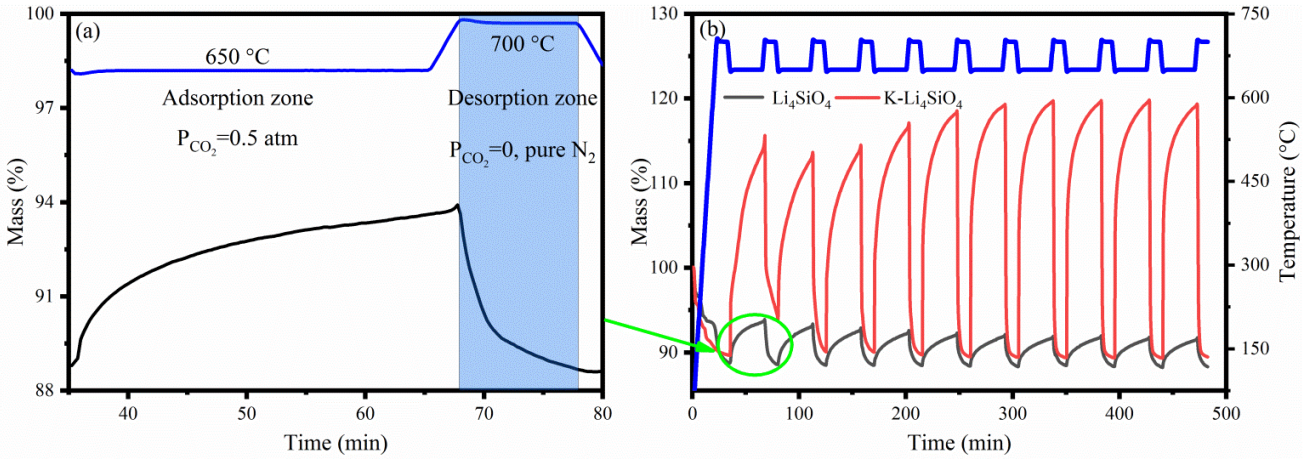

Figure 3. Illustration of (a) the single adsorption/desorption process of Li_4SiO_4, and (b) 10 cycles of adsorption (650 °C, P_{CO_2}=0.5 atm, 30 min) and desorption (700 °C, pure N_2, 10 min).

3.2. Apparent Desorption Kinetics

Global reaction order (n in Eq. 3) reflects the effect exerted by the difference of $(P_{eq}\text{-}P_{CO_2})$ towards the desorption rate, and it can be obtained according to the slope variation in the initial linear stage. Fig. 4 (a, d) depict the desorbing scatter plot of Li_4SiO_4 and K-Li_4SiO_4 at 700 °C, under CO_2 pressure of 0-0.5 atm. It is clear that the regeneration of sorbents reaches a conversion over 0.8 within 200 s when CO_2 pressure is below 0.3 atm, but the reaction rate greatly decreases under 0.4-0.5 atm, especially for K-Li_4SiO_4. This phenomenon reveals that CO_2 pressure has a strong influence on the regeneration rate of Li_4SiO_4-based sorbents. In order to figure out their mathematical correlation, the initial reaction rate towards CO_2 desorption will be obtained according to Eq. 3.

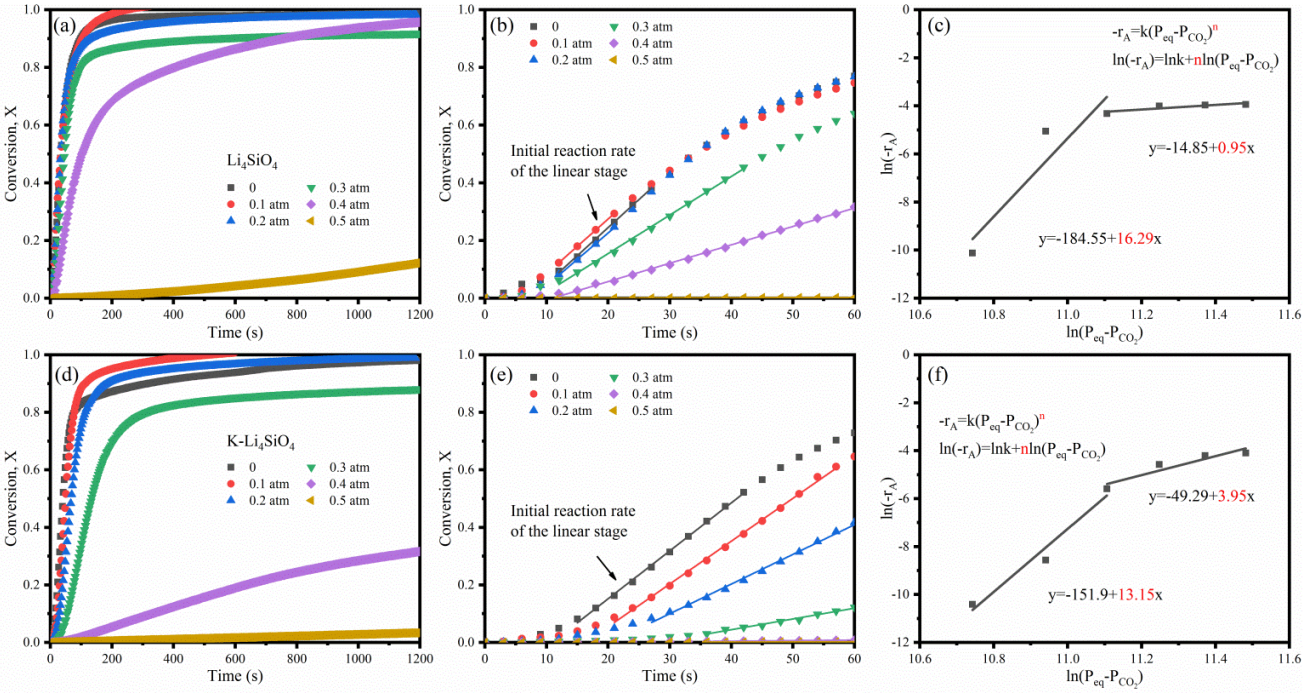

Figure 4. Regeneration plots under different CO_2 pressures at 700 °C, and the determination of reaction order by fitting plots for (a, b, c) Li_4SiO_4 and (d, e, f) K-Li_4SiO_4.

Fig. 4 (b, e) intercepts the original fitting of the scatter plots with straight lines in less than 60 s. Due to the presence of an induction period resulting from gas atmosphere switch during test, the starting point of the linear stage is usually not the origin of coordinates. The initial reaction rates equal the slope of these straight lines. It is noted that for Li_4SiO_4, slopes of the linear stages basically remain unchanged under low CO_2 pressure (0-0.2 atm), but decrease as it rises to 0.3-0.5 atm. While for K-Li_4SiO_4, the slopes

show consecutive decrease with the rise of CO_2 partial pressure. It seems that the regeneration of Li_4SiO_4 is faster than K-Li_4SiO_4 under 0.3-0.5 atm. Although for carbonated K-Li_4SiO_4, more CO_2 is released and transported, but this diffusion effect is eliminated in testing 10 mg sample with particle range of 75-106 μm, according to our previous study *(39, 44)*. It can be verified in the following Fig. 5 (a, d) as well. The reason might be that the release of CO_2 from carbonated K-Li_4SiO_4 is more sensible to $(P_{eq}-P_{CO_2})$. Due to the formation of Li/K eutectic carbonates, more CO_2 is dissolved in eutectics than in solid Li_2CO_3. As the environmental CO_2 pressure reaches 0.3 atm and above, the outward transportation of CO_2 tends to be hindered, resulting in a slower desorption rate.

Fig. 4 (c, f) display the plot of $ln(-r_A)$ versus $ln(P_{eq}-P_{CO_2})$, and the reaction order to $(P_{eq}-P_{CO_2})$ is calculated through linear fitting. Calculation results suggest a reaction order of 1 and 4 under $(P_{eq}-P_{CO_2})$ value of 67-97 kPa, 16 and 13 under 46-67 kPa for Li_4SiO_4 and K-Li_4SiO_4, respectively. Analogously, Sun et al. *(45)* ever reported a nonlinear dependence of the carbonation rate of CaO on the CO_2 pressure when the value of $(P_{eq}-P_{CO_2})$ was higher than 10 kPa.

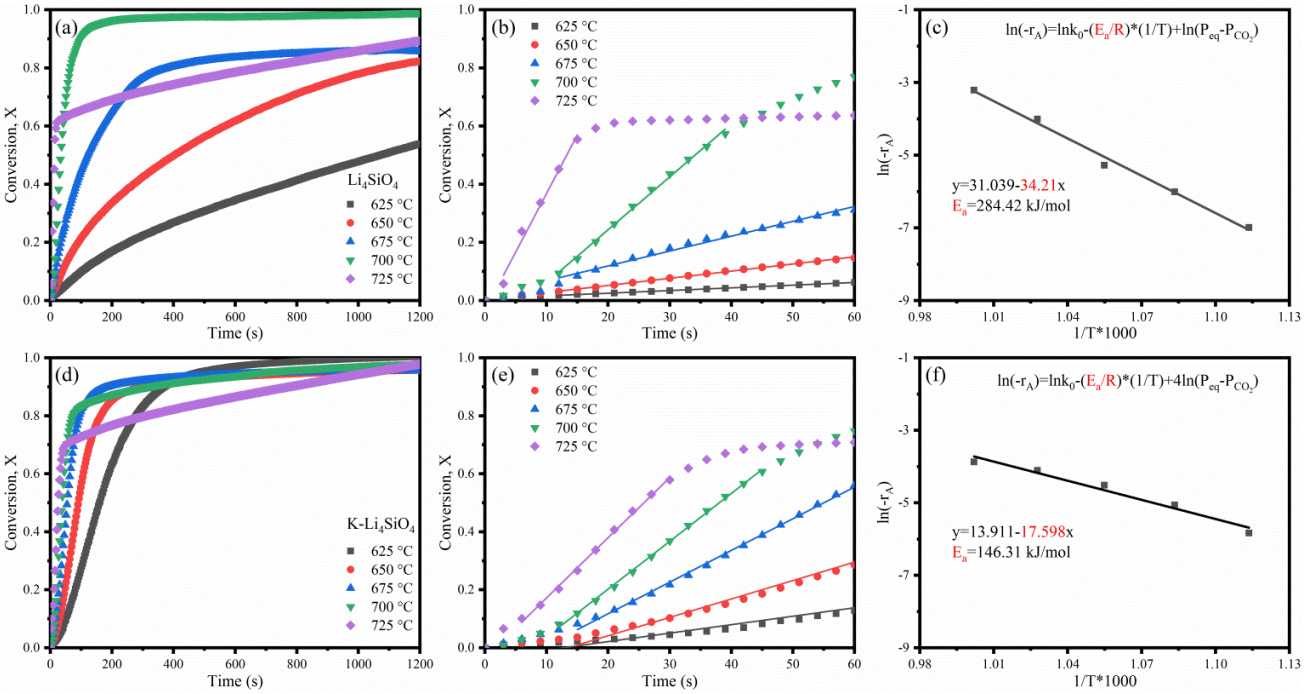

Figure 5. Regeneration plots at different temperatures in pure N_2, and the determination of reaction kinetic parameters by fitting plots for (a, b, c) Li_4SiO_4, and (d, e, f) K-Li_4SiO_4.

Fig. 5 (a, d) show the experimental conversion-time plot for the regeneration of Li_4SiO_4 and K-Li_4SiO_4 under pure N_2 with temperatures varying in 625-725 °C. As can be seen, there are similar change trends of the two sorbents, i.e. along with the rise of temperature, the initial reaction rate becomes larger, and the inflection point between the fast and slow stage appears earlier. In terms of the final conversion rate, it seems that as desorption temperature increases, the conversion rate stabilizes at a higher level, while no such rule is observed for K-Li_4SiO_4. Additionally, regeneration at 725 °C for Li_4SiO_4 behaves distinctively, where the turnover to a slow reaction occurs at a conversion of around 0.6, and then there is a long slow conversion increase to near 1. The similar phenomenon is also observed in the regeneration process of K-Li_4SiO_4. Qi et al. *(10)* reported that the desorption of CO_2 from Li_4SiO_4 at 725 °C was originally controlled by chemical reaction, and then proceeded into diffusion control. It was a result of the liquefaction of Li_2CO_3, whose melting point is 723 °C. Since K_2CO_3-dopant could melt with Li_2CO_3 at a relatively low temperature (~500 °C) to form liquid eutectics *(42, 46)*, the regeneration of K-Li_4SiO_4 at 625-725 °C will be affected. As a result, there is a continuous reduction of the turnover temperature, which indicates the variation from the fast reaction to the slow reaction stage.

Fig. 5 (b, e) intercept the initial desorption curves, and the slope equals the global reaction rate. For both sorbents, there is an induction stage, and the higher the desorbing temperature, the shorter the induction time is. Selection of the starting point of linear stage mainly depends on the exclusion of induction period. It is obvious that global reaction rates of both samples increase along with the rise of temperature. According to the Arrhenius equation, this high temperature-dependent correlation can be depicted through *lnk-1/T* plot, where the linear slope is proportional to the apparent activation energy, as shown in Fig. 5 (c, f). Calculation results show that the apparent activation energy of Li_4SiO_4 and K-Li_4SiO_4 are 284.42 kJ•mol^{-1} and 146.31 kJ•mol^{-1}, respectively, indicating that K_2CO_3-dopant greatly facilitates the CO_2 desorption from Li_4SiO_4-based sorbents, possibly due to the formation of Li/K eutectic carbonates *(42)*. In brief, the regeneration rate of Li_4SiO_4 and K-Li_4SiO_4 as a function of temperature (in unit of K) and CO_2 pressure (in Pa) can be expressed as Eq. (6-9).

For Li_4SiO_4:

$$-r_A = 3.12\times10^{8}\times(P_{eq}-P_{CO_2})\exp(-34210/T)\text{, when } 67\ kPa < P_{eq}-P_{CO_2} \le 97\ kPa \quad (6)$$

$$-r_A = 4.96\times10^{-67}\times(P_{eq}-P_{CO_2})^{16}\exp(-34210/T)\text{, when } 46\ kPa \le P_{eq}-P_{CO_2} \le 67\ kPa \quad (7)$$

For K-Li_4SiO_4:

$$-r_A = 1.25\times10^{-14}\times(P_{eq}-P_{CO_2})^{4}\exp(-17598/T)\text{, when } 67\ kPa < P_{eq}-P_{CO_2} \le 97\ kPa \quad (8)$$

$$-r_A = 1.65\times10^{-59}\times(P_{eq}-P_{CO_2})^{13}\exp(-17598/T)\text{, when } 46\ kPa \le P_{eq}-P_{CO_2} \le 67\ kPa \quad (9)$$

3.3. Analysis by Power Law Model

Power law model contains a series of mechanism functions, with the exponential '*m*' being 2/3, 1/2 or 0 according to the geometry of the grain *(40)*. Other equivalent representations take '*m*' as a reaction order, varying from 0 to 10 *(10, 47)*. Since the simulation accuracy differs along with various values of '*m*', power law model is generally treated as a semi-empirical model. It is worth noting that *m*=2/3 is frequently used to describe the carbonation/calcination of CaO-based sorbents *(37, 38)*, and *m*=2 is reported to fit the carbonation of Li_4SiO_4-based sorbents well *(27)*. Through a preliminary comparison of these power-law formulas with different exponential (*m*), it is found that *m*=4/3 could best cope with the conversion-time plots fitting. Thus the power law model with *m*=4/3 is the most probable mechanism function for the regeneration of Li_4SiO_4-based sorbents. The detailed kinetic parameters and its graphic illustration are presented in this section.

The solid curves in Fig. 6 (a, c) represent the simulation results by power law model basing on experimental dots from 0 to 1200 s, and the modeling parameters are summarized in Table 1. Notably, almost all data fitting possesses good R^2 values, suggesting a good applicability of the power law model with *m*=4/3. The only exception is 725 °C with an abrupt turnover of fast-to-slow stage at conversions of 0.6-0.7. It is very likely to be caused by the liquefaction of Li_2CO_3, as aforementioned. For both sorbents, the value of rate constant (*K*) increases with elevated temperatures from 625 °C to 700 °C, showing a strong temperature dependence. Additionally, the rate constant *K* for the regeneration of K-Li_4SiO_4 is

bigger than Li_4SiO_4 in the range of 625-675 °C, verifying that K_2CO_3 dopants could promote sorbents regeneration in pure N_2 under low temperatures.

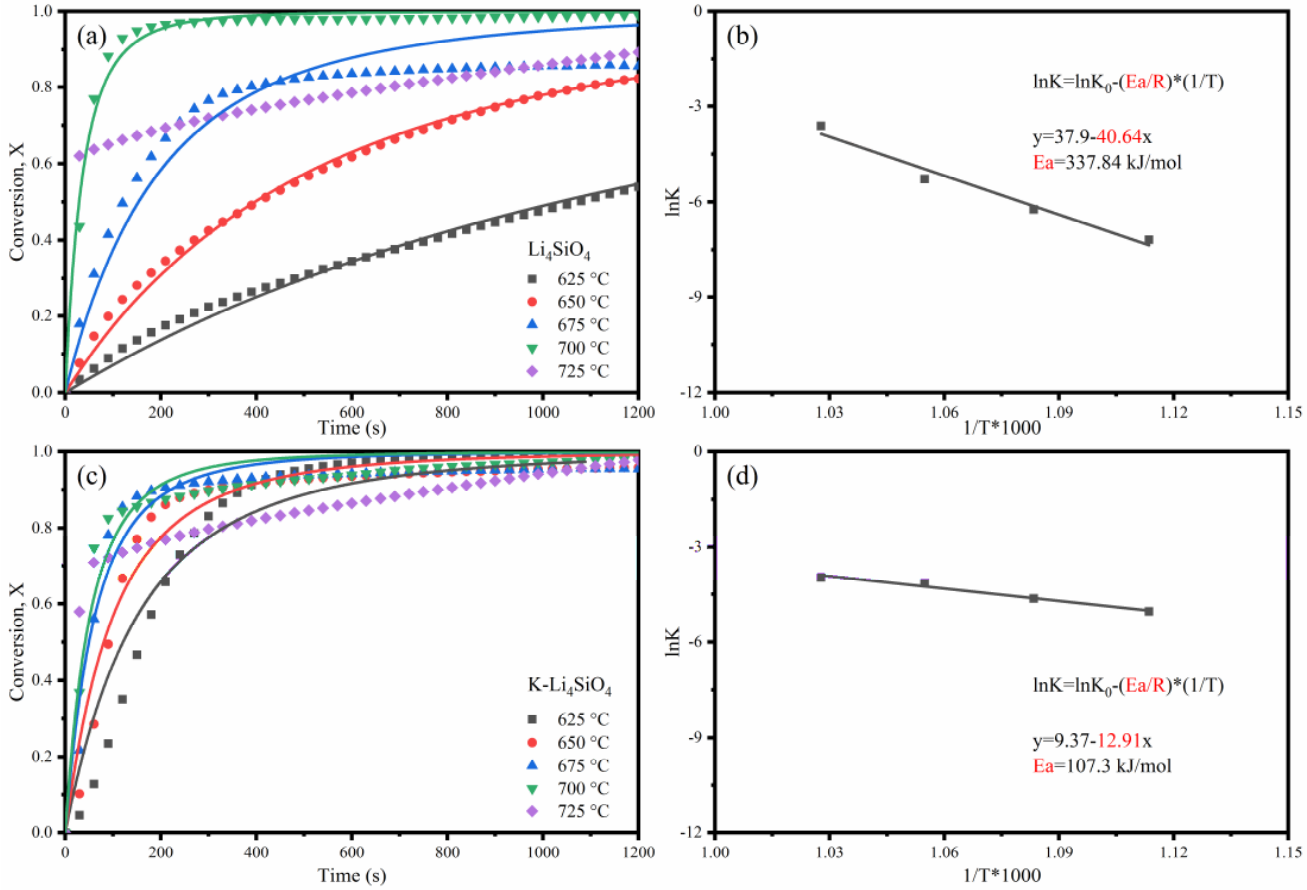

Figure 6. Calculation of intrinsic activation energy for the regeneration of (a, b) Li_4SiO_4 and (c, d) K-Li_4SiO_4 in pure N_2 using power law model (m=4/3).

The intrinsic activation energy is obtained through plotting *lnK* versus *1/T*, according to Arrhenius equation, as depicted in Fig. 6 (b, d). Results show that the intrinsic activation energies for the regeneration of Li_4SiO_4 and K-Li_4SiO_4 are 337.84 kJ•mol^{-1} and 107.3 kJ•mol^{-1}, respectively. It is within the range of the reported 236.9 kJ•mol^{-1} of pure Li_4SiO_4 *(9)* by shrinking core model and 357 kJ•mol^{-1} *(10)* by Avrami-Erofeev model. The variation may be caused by the presence of various impurities in sorbents and the different models used.

Table 1. Parameters for the regeneration of Li_4SiO_4 and K-Li_4SiO_4 in pure N_2, using power law model (m=4/3).

Sorbent	*Temperature (°C)*	*K (s^{-1})*	*R^2*	*E_a ($kJ \cdot mol^{-1}$)*
Li_4SiO_4	625	7.55E-04	0.9973	337.84
	650	1.97E-03	0.9977	
	675	5.09E-03	0.9506	
	700	2.69E-02	0.9711	
	725	5.67E-03	0.7768	/
K-Li_4SiO_4	625	6.47E-03	0.9772	107.3
	650	9.68E-03	0.9559	
	675	1.57E-02	0.9444	
	700	1.88E-02	0.9366	
	725	1.09E-02	0.8107	/

4. Conclusions

This work studied kinetic features of the regeneration process of pure and K-Li4SiO4 under various CO_2 pressures and temperatures, through experiments and data fitting. To sum up, there is a significant negative effect of CO_2 pressure on the regeneration rate of Li_4SiO_4-based sorbents, and we proposed, for the first time, an expression of $(P_{eq}-P_{CO_2})^n$ to account for its dependence on $(P_{eq}-P_{CO_2})$. The most probable mechanism function for Li_4SiO_4 regeneration is determined to be the power law model with m=4/3. In addition, it is found that both apparent and intrinsic activation energies for the regeneration of Li_4SiO_4 are 2-3 times that of K-Li_4SiO_4.

Acknowledgements

The authors are grateful for financial support from National Natural Science Foundation of China (No. 52076020), the Fundamental Research Funds for the Central Universities (No. 2020CDJQY-A050), and Venture and Innovation Support Program for Chongqing Overseas Returnees (No. cx2017021).

References

1 Luo, C.; Zheng, Y.; Ding, N.; Wu, Q.; Bian, G.; Zheng, C., Development and Performance of CaO/La_2O_3 Sorbents during Calcium Looping Cycles for CO_2 Capture. *Ind Eng Chem Res* **2010,** *49* (22), 11778-11784. https://doi.org/10.1021/ie1012745.

2 Ma, X.; Li, Y.; Yan, X.; Zhang, W.; Zhao, J.; Wang, Z., Preparation of a morph-genetic CaO-based sorbent using paper fibre as a biotemplate for enhanced CO_2 capture. *Chem Eng J* **2019,** *361*, 235-244. https://doi.org/https://doi.org/10.1016/j.cej.2018.12.061.

3 Sun, J.; Sun, Y.; Yang, Y. D.; Tong, X. L.; Liu, W. Q., Plastic/rubber waste-templated carbide slag pellets for regenerable CO_2 capture at elevated temperature. *Appl Energ* **2019,** *242*, 919-930. https://doi.org/10.1016/j.apenergy.2019.03.165.

4 Izquierdo, M. T.; Turan, A.; García, S.; Maroto-Valer, M. M., Optimization of Li_4SiO_4 synthesis conditions by a solid state method for maximum CO_2 capture at high temperature. *J Mater Chem A* **2018,** *6* (7), 3249-3257. https://doi.org/10.1039/c7ta08738a.

5 Junya Wang, T. Z., Unexpected Highly Reversible Lithium-Silicate-Based CO_2 Sorbents Derived from Sediment of Dianchi Lake. *Energy Fuels* **2019,** *33* (3), 1734-1744. https://doi.org/10.1021/acs.energyfuels.8b02820.

6 Seggiani, M.; Stefanelli, E.; Puccini, M.; Vitolo, S., CO_2 sorption/desorption performance study on K_2CO_3-doped Li_4SiO_4-based pellets. *Chem Eng J* **2018,** *339*, 51-60. https://doi.org/10.1016/j.cej.2018.01.117.

7 Vallace, A.; Brooks, S.; Coe, C.; Smith, M. A., Kinetic Model for CO_2 Capture by Lithium Silicates. *J Phys Chem C* **2020,** *124* (37), 20506-20515. https://doi.org/10.1021/acs.jpcc.0c04230.

8 Hu, Y.; Liu, W.; Yang, Y.; Qu, M.; Li, H., CO_2 capture by Li_4SiO_4 sorbents and their applications: Current developments and new trends. *Chem Eng J* **2019,** *359*, 604-625. https://doi.org/10.1016/j.cej.2018.11.128.

9 Amorim, S. M.; Domenico, M. D.; Dantas, T. L. P.; José, H. J.; Moreira, R. F. P. M., Lithium orthosilicate for CO_2 capture with high regeneration capacity: Kinetic study and modeling of carbonation and decarbonation reactions. *Chem Eng J* **2016,** *283*, 388-396. https://doi.org/10.1016/j.cej.2015.07.083.

10 Qi, Z.; Daying, H.; Yang, L.; Qian, Y.; Zibin, Z., Analysis of CO_2 sorption/desorption kinetic behaviors and reaction mechanisms on Li_4SiO_4. *Aiche J* **2013,** *59* (3), 901-911. https://doi.org/10.1002/aic.13861.

11 Stefanelli, E.; Puccini, M.; Vitolo, S.; Seggiani, M., CO_2 sorption kinetic study and modeling on doped-Li_4SiO_4 under different temperatures and CO_2 partial pressures. *Chem Eng J* **2020,** *379*. https://doi.org/10.1016/j.cej.2019.122307.

12 Ma, L.; Chen, S. Z.; Qin, C. L.; Chen, S. S.; Yuan, W. Y.; Zhou, X.; Ran, J. Y., Understanding the effect of H_2S on the capture of CO_2 using K-doped Li_4SiO_4 sorbent. *Fuel* **2021,** *283*. https://doi.org/10.1016/j.fuel.2020.119364.

13 Zhang, S.; Zhang, Q.; Wang, H.; Ni, Y.; Zhu, Z., Absorption behaviors study on doped Li_4SiO_4 under a humidified atmosphere with low CO_2 concentration. *Int J Hydrogen Energ* **2014,** *39* (31), 17913-17920. https://doi.org/10.1016/j.ijhydene.2014.07.011.

14 Pacciani, R.; Torres, J.; Solsona, P.; Coe, C.; Quinn, R.; Hufton, J.; Golden, T.; Vega, L. F., Influence of the Concentration of CO_2 and SO_2 on the Absorption of CO_2 by a Lithium Orthosilicate-Based Absorbent. *Environ. Sci. Technol.* **2011,** *45* (16), 7083-7088. https://doi.org/10.1021/es201269j.

15 Qin, C. L.; He, D. L.; Zhang, Z. H.; Tan, L. L.; Ran, J. Y., The consecutive calcination/sulfation in calcium looping for CO_2 capture: Particle modeling and behaviour investigation. *Chem Eng J* **2018,** *334*, 2238-2249. https://doi.org/10.1016/j.cej.2017.11.169.

16 He, D. L.; Ou, Z. L.; Qin, C. L.; Deng, T.; Yin, J. J.; Pu, G., Understanding the catalytic acceleration effect of steam on $CaCO_3$ decomposition by density function theory. *Chem Eng J* **2020,** *379*. https://doi.org/10.1016/j.cej.2019.122348.

17 López Ortiz, A.; Escobedo Bretado, M. A.; Guzmán Velderrain, V.; Meléndez Zaragoza, M.; Salinas Gutiérrez, J.; Lardizábal Gutiérrez, D.; Collins-Martínez, V., Experimental and modeling kinetic study of the CO_2 absorption by Li_4SiO_4. *Int J Hydrogen Energ* **2014,** *39* (29), 16656-16666. https://doi.org/10.1016/j.ijhydene.2014.05.015.

18 Izquierdo, M. T.; Gasquet, V.; Sansom, E.; Ojeda, M.; Garcia, S.; Maroto-Valer, M. M., Lithium-based sorbents for high temperature CO_2 capture: Effect of precursor materials and synthesis method. *Fuel* **2018,** *230*, 45-51. https://doi.org/10.1016/j.fuel.2018.05.041.

19 Lee, J. S.; Yavuz, C. T., Enhanced Sorption Cycle Stability and Kinetics of CO_2 on Lithium Silicates Using the Lithium Ion Channeling Effect of TiO_2 Nanotubes. *Industrial and Engineering Chemistry Research* **2017,** *56* (12), 3413-3417. https://doi.org/10.1021/acs.iecr.6b04918.

20 Wang, K.; Zhou, Z. Y.; Zhao, P. F.; Yin, Z. G.; Su, Z.; Sun, J., Synthesis of a highly efficient Li_4SiO_4 ceramic modified with a gluconic acid-based carbon coating for high-temperature CO_2 capture. *Appl Energ* **2016,** *183*, 1418-1427. https://doi.org/10.1016/j.apenergy.2016.09.105.

21 Ma, L.; Qin, C. L.; Pi, S.; Cui, H. N., Fabrication of efficient and stable Li_4SiO_4-based sorbent pellets via extrusion-spheronization for cyclic CO_2 capture. *Chem Eng J* **2020,** *379*. https://doi.org/10.1016/j.cej.2019.122385.

22 Li, H.; Qu, M.; Hu, Y., Preparation of spherical Li_4SiO_4 pellets by novel agar method for high-temperature CO_2 capture. *Chem Eng J* **2020,** *380*. https://doi.org/10.1016/j.cej.2019.122538.

23 Yang, Y. D.; Liu, W. Q.; Hu, Y. C.; Sun, J.; Tong, X. L.; Chen, Q. J.; Li, Q. W., One-step synthesis of porous Li_4SiO_4-based adsorbent pellets via graphite moulding method for cyclic CO_2 capture. *Chem Eng J* **2018,** *353*, 92-99. https://doi.org/10.1016/j.cej.2018.07.044.

24 Kato, M.; Yoshikawa, S.; Nakagawa, K., Carbon dioxide absorption by lithium orthosilicate in a wide range of temperature and carbon dioxide concentrations. *Journal of Materials Science Letters* **2002,** *21* (6), 485-487. https://doi.org/Doi 10.1023/A:1015338808533.

25 Hu, Y.; Liu, W.; Yang, Y.; Tong, X.; Chen, Q.; Zhou, Z., Synthesis of highly efficient, structurally improved Li_4SiO_4 sorbents for high-temperature CO_2 capture. *Ceram Int* **2018,** *44* (14), 16668-16677. https://doi.org/10.1016/j.ceramint.2018.06.094.

26 Venegas, M. J.; Fregoso-Israel, E.; Escamilla, R.; Pfeiffer, H., Kinetic and Reaction Mechanism of CO_2 Sorption on Li_4SiO_4: Study of the Particle Size Effect. *Ind Eng Chem Res* **2007,** *46* (8), 2407-2412. https://doi.org/10.1021/ie061259e.

27 Rusten, H. K.; Ochoa-Fernández, E.; Lindborg, H.; Chen, D.; Jakobsen, H. A., Hydrogen Production by Sorption-Enhanced Steam Methane Reforming Using Lithium Oxides as CO_2-Acceptor. *Ind Eng Chem Res* **2007,** *46* (25), 8729-8737. https://doi.org/10.1021/ie070770k.

28 Takasu, H.; Funayama, S.; Uchiyama, N.; Hoshino, H.; Tamura, Y.; Kato, Y., Kinetic analysis of the carbonation of lithium orthosilicate using the shrinking core model. *Ceram Int* **2018,** *44* (10), 11835-11839. https://doi.org/10.1016/j.ceramint.2018.03.273.

29 Zhang, Q., Behaviors And Kinetic Models Analysis Of Li_4SiO_4 Under Various CO_2 Partial Pressures. *Aiche J* **2017,** *63* (6), 2153-2164. https://doi.org/10.1002/aic.15627.

30 Quddus, M. R.; Chowdhury, M. B. I.; de Lasa, H. I., Non-isothermal kinetic study of CO_2 sorption and desorption using a fluidizable Li_4SiO_4. *Chem Eng J* **2015,** *260*, 347-356. https://doi.org/10.1016/j.cej.2014.08.055.

31 Li, H. L.; Qu, M. Y.; Hu, Y. C., High-temperature CO_2 capture by Li_4SiO_4 adsorbents: Effects of pyroligneous acid (PA) modification and existence of CO_2 at desorption stage. *Fuel Process Technol* **2020,** *197*. https://doi.org/10.1016/j.fuproc.2019.106186.

32 Ortiz-Landeros, J.; Avalos-Rendon, T. L.; Gomez-Yanez, C.; Pfeiffer, H., Analysis and perspectives concerning CO_2 chemisorption on lithium ceramics using thermal analysis. *Journal of Thermal Analysis and Calorimetry* **2012,** *108* (2), 647-655. https://doi.org/10.1007/s10973-011-2063-y.

33 Kato, M.; Nakagawa, K.; Essaki, K.; Maezawa, Y.; Takeda, S.; Kogo, R.; Hagiwara, Y., Novel CO_2 absorbents using lithium-containing oxide. *International Journal of Applied Ceramic Technology* **2005,** *2* (6), 467-475. https://doi.org/10.1111/j.1744-7402.2005.02047.x.

34 Jun-Ichi, I.; Lin, Y. S., Mechanism of High-Temperature CO_2 Sorption on Lithium Zirconate. *Environ. Sci. Technol.* **2003,** *37* (9), 1999. https://doi.org/10.1021/es0259032.

35 Rodríguez-Mosqueda, R.; Pfeiffer, H., Thermokinetic Analysis of the CO_2 Chemisorption on Li_4SiO_4 by Using Different Gas Flow Rates and Particle Sizes. *The Journal of Physical Chemistry A* **2010,** *114* (13), 4535-4541. https://doi.org/10.1021/jp911491t.

36 Jander, W., Reactions in solid states at room temperature I Announcement the rate of reaction in endothermic conversions. *Zeitschrift Fur Anorganische Und Allgemeine Chemie* **1927,** *163* (1/2), 1-30. https://doi.org/10.1002/zaac.19271630102.

37 Kyaw, K.; Kanamori, M.; Matsuda, H.; Hasatani, M., Study of Carbonation Reactions of Ca-Mg Oxides for High Temperature Energy Storage and Heat Transformation. *JOURNAL OF CHEMICAL ENGINEERING OF JAPAN* **1996,** *29* (1), 112-118. https://doi.org/10.1252/jcej.29.112.

38 Fang, F.; Li, Z.-S.; Cai, N.-S., Experiment and Modeling of CO_2 Capture from Flue Gases at High Temperature in a Fluidized Bed Reactor with Ca-Based Sorbents. *Energ Fuel* **2009,** *23* (1), 207-216. https://doi.org/10.1021/ef800474n.

39 Chen, S. Z.; Dai, J. Z.; Qin, C. L.; Yuan, W. Y.; Manovic, V., Adsorption and Desorption Equilibrium of Li_4SiO_4-based Sorbents for High-temperature CO_2 Capture. *Chem Eng J* **(in press)**.

40 Bhatia, S. K.; Perlmutter, D. D., A random pore model for fluid-solid reactions: I. Isothermal, kinetic control. *Aiche J* **1980,** *26* (3), 379-386. https://doi.org/https://doi.org/10.1002/aic.690260308.

41 Zheng, J.-c.; Yang, Z.; He, Z.-j.; Tong, H.; Yu, W.-j.; Zhang, J.-f., In situ formed $LiNi_{0.8}Co_{0.15}Al_{0.05}O_2$@$Li_4SiO_4$ composite cathode material with highratecapability and long cycling

stability for lithium-ion batteries. *Nano Energy* **2018,** *53*, 613-621. https://doi.org/https://doi.org/10.1016/j.nanoen.2018.09.014.

42 Cui, H.; Li, X.; Chen, H.; Gu, X.; Cheng, Z.; Zhou, Z., Sol-gel derived, Na/K-doped Li_4SiO_4-based CO_2 sorbents with fast kinetics at high temperature. *Chem Eng J* **2020,** *382*, 122807. https://doi.org/10.1016/j.cej.2019.122807.

43 Kruk, M.; Jaroniec, M., Gas Adsorption Characterization of Ordered Organic−Inorganic Nanocomposite Materials. *Chemistry of Materials* **2001,** *13* (10), 3169-3183. https://doi.org/10.1021/cm0101069.

44 Chen, S.; Qin, C.; Yin, J.; Zhou, X.; Chen, S.; Ran, J., Understanding sulfation effect on the kinetics of carbonation reaction in calcium looping for CO_2 capture. *Fuel Process Technol* **2021,** *221*, 106913. https://doi.org/https://doi.org/10.1016/j.fuproc.2021.106913.

45 Sun, P.; Grace, J. R.; Lim, C. J.; Anthony, E. J., Determination of intrinsic rate constants of the CaO–CO_2 reaction. *Chemical Engineering Science* **2008,** *63* (1), 47-56. https://doi.org/https://doi.org/10.1016/j.ces.2007.08.055.

46 Yang, X.; Liu, W.; Sun, J.; Hu, Y.; Wang, W.; Chen, H.; Zhang, Y.; Li, X.; Xu, M., Alkali-Doped Lithium Orthosilicate Sorbents for Carbon Dioxide Capture. *ChemSusChem* **2016,** *9* (17), 2480-2487. https://doi.org/10.1002/cssc.201600737.

47 Ishida, M.; Wen, C. Y., Comparison of zone-reaction model and unreacted-core shrinking model in solid—gas reactions—I isothermal analysis. *Chemical Engineering Science* **1971,** *26* (7), 1031-1041. https://doi.org/https://doi.org/10.1016/0009-2509(71)80017-9.